Vertically coupled double quantum dots in magnetic fields

Hiroshi Imamura
CREST and Institute for Materials Research, Tohoku University, Sendai 980-8577, Japan

Peter A. Maksym
Department of Physics and Astronomy, University of Leicester, Leicester LE1 7RH, United Kingdom

Hideo Aoki
Department of Physics, University of Tokyo, Hongo, Tokyo 113-0033, Japan
(Received 12 October 1998)

Ground- and excited-state properties of vertically coupled double quantum dots are studied by exact diagonalization. Magic-number total angular momenta that minimize the total energy are found to reflect a crossover between electron configurations dominated by intralayer correlation and those dominated by interlayer correlation. The position of the crossover is governed by the strength of the interlayer electron tunneling and magnetic field. The magic numbers should have an observable effect on the far-infrared optical-absorption spectrum, since Kohn's theorem [Phys. Rev. **123**, 1242 (1961)] does not hold when the confinement potential is different for two dots. This is indeed confirmed here from a numerical calculation that includes Landau-level mixing. Our results take full account of the effect of spin degrees of freedom. A key feature is that the total spin S of the system and the magic-number angular momentum are intimately linked because of strong electron correlation. Thus S jumps hand in hand with the total angular momentum as the magnetic field is varied. One important consequence of this is that the spin blockade (an inhibition of single-electron tunneling) should occur in some magnetic field regions because of a spin selection rule. Owing to the flexibility arising from the presence of both intralayer and interlayer correlations, the spin blockade is easier to realize in double dots than in single dots. [S0163-1829(99)04408-2]

I. INTRODUCTION

Vertically coupled quantum dots have recently attracted much interest, since they open up the possibility of manipulating electron configurations in three-dimensional space. Quantum dots are generally thought of as ''artificial atoms,'' in which electrons are confined by an artificial electrostatic potential instead of being attracted to a nucleus. Numerical studies of few-electron systems confined in single quantum dots have shown that the angular momentum and spin of the ground state in strong magnetic fields belong to a special series values called magic numbers. For single quantum dots the interval of magic number angular momenta has a one-to-one correspondence with the symmetry of charge correlation. This has been explained by an ''electron-molecule'' picture by one of the present authors.[1] That is, the Coulomb repulsion forces the electrons confined in a dot to take a definite molecular configuration (triangle for three electrons, square for four, etc.) when the electron correlation is strong.[1,2] If we use a similar picture for vertically coupled dots we can envisage the ground states in strong magnetic fields as three-dimensional electron molecules.

On the experimental side, recent advances in nanolithography and thin-film processing make it possible to fabricate vertically coupled multiple quantum dots, where two-dimensional (2D) electrons are confined within an area smaller than 1 μm across.[3] Observable effects in the atom-like physics of dots have been detected from measurements of the tunneling current or capacitance. In the low-magnetic-field regime ($B \leqslant 2$ T), Tarucha, Austing, and Honda indeed found from capacitance spectroscopy that Hund's rule and shell structures appear in the spectrum.[4] As the magnetic field becomes stronger, however, the single-electron energy levels change to ones like those of a 2D harmonic oscillator to Landau levels, where levels with different angular momenta are degenerate, and electron correlation should play an essential role. Ashoori *et al.* and Wagner, Merkt, and Chaplik looked at the addition spectrum (energies required for adding one additional electron) for single dots in magnetic fields, where a total-spin transition caused by the Coulomb interaction is expected.[5–7]

This reminds us of the fractional quantum Hall effect (FQHE) in the bulk 2D electron system, a manifestation of strong electron correlation in high magnetic fields,[8–10] where the total spin is a sensitive function of the density of electrons in the Landau levels. This is an effect of electron correlation, i.e., the way the electrons are correlated is strongly dominated by the total spin, while the Zeeman energy, which is few percent of the typical Coulomb energy, has only a minor effect.

The fractional quantum Hall effect in double layers[11–16] has recently been under intense study. In this case the additional degree of freedom arising from the double layer (a pseudospin that labels the layers) enriches the physics. A central issue in these systems is the interplay of electron correlation and interlayer electron tunneling. The competition between these effects makes the quantum Hall state evolve continuously from a correlation-dominated (two-component) state to a tunneling-dominated (single-component) state within the quantum Hall regime. If we in-

clude spin degrees of freedom, FQH states specific to double-layer systems of electrons with certain specific spins indeed appear.[13] Thus vertically coupled quantum dots are also intriguing from the viewpoint of what happens if we laterally confine a double-layer FQH system.

In the present paper we investigate the physics of double dots in magnetic fields. While we studied the magic numbers and far infrared (FIR) absorption in our previous publications,[17,18] we assumed there that the system is fully spin polarized (except for our paper on the spin blockade, as recapitulated here in Sec. V). We also adopted the lowest Landau-level approximation there. These assumptions, however, are justified only for $B\rightarrow\infty$ limit.

One of our most important findings is that the total spin of the ground state of the dots changes wildly as the magnetic field varies, where the ground state is spin *un*polarized even for a magnetic field as large as $B=4$ T in typical conditions. We show that this is a manifestation of electron correlation rather than the spin Zeeman effect. That is, the electron correlation energy is drastically affected by the total spin state even when we ignore the Zeeman term, so that it is the former that determines the spin. A similar phenomenon occurs in single dots, and is explained by the electron-molecule theory that takes care of spin quantum numbers.[1,2] The wild change in the spin can cause single-electron tunneling to be blocked in some magnetic-field regimes due to spin selection rules, as we have recently proposed.[19] Evidence that this effect is caused by electron correlation is the occurrence of a reentrant nonblocked region which is hard to explain by Zeeman-energy considerations.

We have also investigated the effect of the difference in the curvature of the confinement potential in the two layers. This can be regarded as a pseudospin Zeeman energy, and a charge correlation caused by the pseudospin Zeeman energy is found to appear, which causes a dependence of the magic numbers on the strength of the interdot electron tunneling and the layer separation. The upper branch in the absorption spectrum that approaches the cyclotron frequency for large B has been obtained from a calculation that includes higher Landau levels. We propose that the magic numbers should have an observable effect on both the higher and lower branches of the FIR spectrum. Specifically, while the generalized Kohn theorem[20,21] states that the electron correlation cannot affect the optical-absorption spectra in single dots with parabolic confinement, this is no longer the case with vertically coupled dots that have different confining potentials. We show that the absorption energy of the double dot should indeed exhibit discontinuities at the magnetic fields where the total angular momentum or total spin change from one magic number to another.

Thus the purpose of this paper is twofold: to include the spin degrees of freedom and to include the mixing of higher Landau levels, which enables us to calculate the real ground state. The magic numbers in double dots are found to depend on the strength of the interdot tunneling and this determines how the total spin (S) changes hand in hand with the total angular momentum (L), which can be distinct from the link between S and L in single dots.

The organization of this paper is as follows: In Sec. II the theoretical model of a vertically coupled quantum dot is described. The physics of electron correlation in double dots and its relevance to the magic numbers is discussed in Sec. III. The remaining sections deal with the experimental consequences of our results. All the results are summarized in Sec. VI.

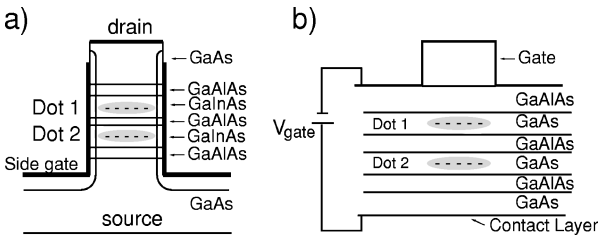

FIG. 1. A deep-mesa etched (gated) vertically coupled quantum dot is shown schematically in (a) [(b)].

II. VERTICALLY COUPLED QUANTUM DOTS

Quantum dots are fabricated with a variety of techniques. The difference between these techniques lies in the way the lateral confinement potential of a two-dimensional electron system is created. One method for obtaining lateral confinement is to etch away a semiconductor sample to obtain mesas which contain a laterally confined two-dimensional electron system. The dot structure fabricated in this way is called a ''deep-mesa-etched'' quantum dot [Fig. 1(a)]. Another method is to deposit a metallic gate on top of a heterostructure. When biased negatively the gate will deplete electrons from the region underneath it, thereby creating a quantum dot [Fig. 1(b)]. Simple electrostatic considerations show that the potential ''felt'' by an electron in a mesa-etched sample is similar to that of a charged disk. The electrostatic potential of a charged disk can be found in terms of elliptic integrals, and the bottom of the potential is well approximated by a parabola.[21,22]

Recent advances in semiconductor fabrication techniques have enabled the fabrication of double dots in vertical, triple-barrier structures on submicron scales. Figure 1(a) actually depicts such a case: a gated field-effect-confined double dot and a deep-mesa-etched double dot with the source gate on top, which was studied in Ref. 23.

As mentioned, we can assume that the confining potential of a quantum dot is parabolic. Then the single-electron states are those of a two-dimensional harmonic oscillator. When a

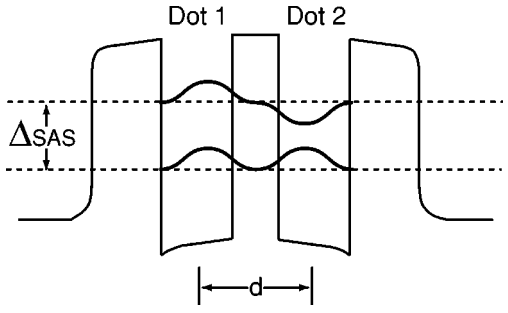

FIG. 2. Schematic single-electron wave functions in the direction normal to the layers in a double quantum dot.

perpendicular magnetic field B is applied, the Hamiltonian for a single electron in a quantum dot is given by

$$\mathcal{H}=\frac{1}{2m^*}\boldsymbol{\pi}^2+\frac{1}{2}m^*\omega_0^2 r^2+\frac{1}{2}g^*\mu_B B\sigma_z, \tag{1}$$

where m^* is the effective mass, ω_0 is the strength of the parabolic confinement potential, μ_B is the Bohr magneton, g^* is the effective g factor, $\frac{1}{2}\sigma_z$ is the z component of the spin of a single electron, and the canonical momentum $\boldsymbol{\pi}$ is given by

$$\boldsymbol{\pi}=-i\hbar\boldsymbol{\nabla}+e\mathbf{A}, \tag{2}$$

where the vector potential $\mathbf{A}$ satisfies $\boldsymbol{\nabla}\times\mathbf{A}=\mathbf{B}$. For parabolic confinement, the Hamiltonian is similar to that for a free electron, so that the eigenstates ϕ_{nl}, called Fock-Darwin states,[24,25] are given by

$$\phi_{nl}(\mathbf{r})=\sqrt{\frac{n!}{2\pi\lambda^2 2^{|l|}\lambda^{2|l|}(n+|l|)!}}\,r^{|l|}e^{-il\theta}L_n^{|l|}\left(\frac{r^2}{2\lambda^2}\right)\exp\left(-\frac{r^2}{4\lambda^2}\right). \tag{3}$$

Here n is the radial quantum number, l is the angular momentum quantum number, $L_n^{|l|}$ is a Laguerre polynomial, $\lambda=\sqrt{\hbar/m^*\Omega}$ is the effective magnetic length, $\Omega\equiv\sqrt{\omega_c^2+4\omega_0^2}$, and $\omega_c=eB/m^*$ is the cyclotron frequency. The Fock-Darwin states are ring shaped, with a radius $R\sim\lambda\sqrt{2(2n+|l|+1)}$. The eigenenergies are given by

$$E_{nl\sigma}(\Omega)=\tfrac{1}{2}(2n+1+|l|)\hbar\Omega-\tfrac{1}{2}l\hbar\omega_c+\tfrac{1}{2}g^*\mu_B B\sigma_z. \tag{4}$$

For double-quantum-dot systems, the single-electron states are split into symmetric and antisymmetric states due to interlayer tunneling (Fig. 2). The strength of the tunneling is characterized by the energy gap Δ_{SAS} between symmetric and antisymmetric states. Although Δ_{SAS} depends (approximately exponentially) on the layer separation (d), it also depends on the height of the barrier that separates the two layers. Experimentally, d and Δ_{SAS} are independently adjustable. We can see that d controls the difference between the intralayer interaction, $\propto 1/r$, and the interlayer interaction, $\propto 1/(r^2+d^2)^{1/2}$.

The Hamiltonian for interacting electrons in a vertically coupled quantum dot,

$$\mathcal{H}=\mathcal{H}_0+\mathcal{H}_t+\mathcal{H}_C, \tag{5}$$

comprises the single-electron part $\mathcal{H}_0$ and the Coulomb interaction $\mathcal{H}_C$. In second-quantized form with a Fock-Darwin basis, we have

$$\mathcal{H}_0=\sum_n\sum_l\sum_\sigma\sum_\alpha \varepsilon_{nl\sigma\alpha}c^\dagger_{nl\sigma\alpha}c_{nl\sigma\alpha}, \tag{6}$$

$$\mathcal{H}_t=-\frac{\Delta_{\mathrm{SAS}}}{2}\sum_n\sum_l\sum_\sigma (c^\dagger_{nl\sigma+}c_{nl\sigma-}+c^\dagger_{nl\sigma-}c_{nl\sigma+}), \tag{7}$$

$$\mathcal{H}_c=\tfrac{1}{2}\sum_{n_1\sim n_4}\sum_{l_1\sim l_4}\sum_{\sigma_1\sim\sigma_4}\sum_{\alpha_1\sim\alpha_4}\langle n_1 l_1\sigma_1\alpha_1, n_2 l_2\sigma_2\alpha_2|V(\mathbf{r}_1-\mathbf{r}_2)|n_3 l_3\sigma_3\alpha_3, n_4 l_4\sigma_4\alpha_4\rangle \times c^\dagger_{n_1 l_1\sigma_1\alpha_1}c^\dagger_{n_2 l_2\sigma_2\alpha_2}c_{n_4 l_4\sigma_4\alpha_4}c_{n_3 l_3\sigma_3\alpha_3}. \tag{8}$$

Here σ is the real spin, $\alpha=\pm$ is a pseudospin index specifying the two layers, $c^\dagger_{nl\sigma\alpha}$ ($c_{nl\sigma\alpha}$) are creation (annihilation) operators, and ϵ is the dielectric constant of the host material. When the spin and pseudospin are included, the energy of the single-particle states becomes

$$\varepsilon_{nl\sigma\alpha}=E_{nl\sigma}(\Omega_\alpha), \tag{9}$$

where $E_{nl\sigma}$ is given by Eq. (4) and $\Omega_\alpha=(\omega_c^2+4\omega_{0\alpha}^2)^{1/2}$, with $\omega_{0\alpha}$ the confining potential for the αth layer. Because the Coulomb interaction conserves the total angular momentum, the many-body Hamiltonian is diagonalized numerically in each sector of the total angular momentum space.[21,26–29]

III. MAGIC-NUMBER STATES

One of the most dramatic features of interacting two-dimensional electron systems confined in quantum dots subjected to magnetic fields appears in their energy spectrum. Numerical studies of finite single-layer systems have shown that ground states only occur at certain total angular momenta and total spins called ''magic numbers.'' The reason why magic numbers appear is that the Coulomb part of the total energy is not a smooth function of the total angular momentum, L, but has a series of cusps caused by electron correlation.[21] A larger L corresponds to a larger spatial extent ($\sim\sqrt{L}$) of the charge density, which costs a higher confinement-potential energy (Fock-Darwin energy), while the Coulomb repulsion tends to be reduced. What the magic

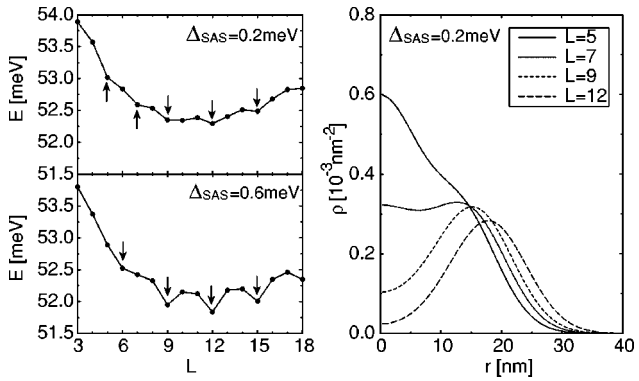

FIG. 3. Left: Ground-state energy against the total angular momentum, L, in vertically coupled dots with three spin-polarized electrons for $\Delta_{\mathrm{SAS}}=0.2$ (0.6) meV at $B=15$ T in the upper (lower) panel. The confinement energy is $\hbar\omega_0=3.0$ meV for both layers, and the layer separation is $d=20$ nm. Arrows indicate the positions of the cusps. Right: Charge density (ρ) per electron for each layer for $L=5$ and 7 (belonging to period 2) and $L=9$ and 12 (period three) with $\Delta_{\mathrm{SAS}}=0.2$ meV.

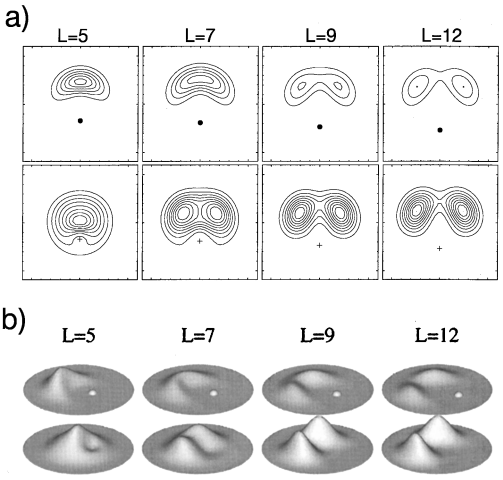

FIG. 4. (a): Contour plot of intralayer (upper panels) and interlayer (lower panels) pair-correlation functions, $P(\mathbf{r},\mathbf{r}_0)$, for $L=5$, 7, 9, and 12. One electron (filled circle) is fixed at the place where the charge density has a maximum in the upper layer. Thus the total charge is $\frac{1}{2}$ ($\frac{3}{2}$) in the upper (lower) layer, since we have $\frac{3}{2}+\frac{3}{2}$ electrons, while we fix one electron in the upper layer. An area with a linear dimension of $12\lambda=78.5$ nm (λ is the effective magnetic length) is displayed. The confinement energies, the layer separation Δ_{SAS}, and $B=15$ T are the same as in Fig. 3. (b) Bird's eye view plot of (a). A white sphere indicates the position of the fixed electron.

numbers are all about is that the competition between these effects is not monotonic. Indeed, the magic numbers have a one-to-one correspondence with the symmetry of charge correlation, which has turned out to be the same as the symmetry of the classical equilibrium configuration of point charges for single dots. If we further take account of the electron spins, we have to consider, in addition to the Zeeman energy, the competition among the states having various total spins that determines how the electrons should be correlated.

Magic number states also occur in double dots. For double dots, however, we have the pseudospin as an additional degree of freedom, which makes the sequence of magic numbers for double dots different from that of single dots. We first look at how the sequence of magic numbers is modified by the strength of the interlayer tunneling.

A. Three-electron double dots

For simplicity we start with three fully spin-polarized electrons in a double dot with the same confining potential for both layers, while the effect of spin will be examined later. We plot the ground-state energy (Fig. 3) calculated numerically as a function of the total angular momentum, L, at $B=15$ T for $\Delta_{\mathrm{SAS}}=0.2$ (0.6) meV in the upper (lower) panel. The confinement energy is $\hbar\omega_0=3.0$ meV for both layers and the layer separation $d=20$ nm.

Magic numbers can be identified from the positions of downward cusps. For $\Delta_{\mathrm{SAS}}=0.2$ meV we have a period of 2 ($L=5$, 7, and 9) for smaller L followed by a period of 3 ($L=9$, 12, ...). For a larger $\Delta_{\mathrm{SAS}}=0.6$ meV, by contrast, the period is 3 for all L, as in the case of a single-dot containing three electrons.

In the right panel of Fig. 3 we show the average charge density ρ, which is axially symmetric. Since we assume the same confinement potential for the two dots, ρ is the same for the two dots. For $L=5$ (solid line) the density against the lateral distance r from the center has a peak at the center along with a shoulder around 11 nm ($=1.7\lambda$; λ: effective magnetic length is 6.54 nm). For $L=12$ belonging to the period of 3 (long dashed line), on the other hand, the density is peaked at a finite r.

In order to identify the mechanism for the change of period in the magic numbers, a better measure of the electron correlation is the pair-correlation function $P(\mathbf{r},\mathbf{r}_0)$, which is proportional to the conditional probability of finding an electron at position $\mathbf{r}$ given that there is one at position $\mathbf{r}_0$. This is shown in Fig. 4. We fixed one electron at the place where the charge density has a shoulder (or a maximum when the density is peaked at a finite r). We can immediately see that the ground-state electron configuration changes from one dominated by interlayer correlation to one dominated by intralayer correlation. In particular, the correlation for $L=5$ corresponds to a triangular ''electron molecule'' developed *across* the two layers, with one electron at the center of the lower layer and the other two in the upper layer. In contrast, the triangular form develops within each layer for $L=9$ and 12. The $L=7$ state is an intermediate one, where the upper layer has a single peak but the lower layer has two peaks.

An important difference between a single and double dot is the way a magnetic field affects the plot of ground-state energy E against L. For single dots and strong fields, such that states with $n=0$ and $l\geqslant 0$ are dominant, the Fock-Darwin energy in Eq. (4) becomes $\hbar(\Omega-\omega_c)l/2+\hbar\Omega/2$. The main effect of changing the magnetic field is then to change the coefficient of the term linear in l so that once we obtain an $E-L$ plot for a specific value of B we can predict how the ground state L will evolve with B. In other words, a series of cusps (magic numbers) in the $E-L$ plot will sequentially become the true ground state as B is varied. For double dots a change in B affects not only the linear term but also the ratio of the effective magnetic length λ and the layer

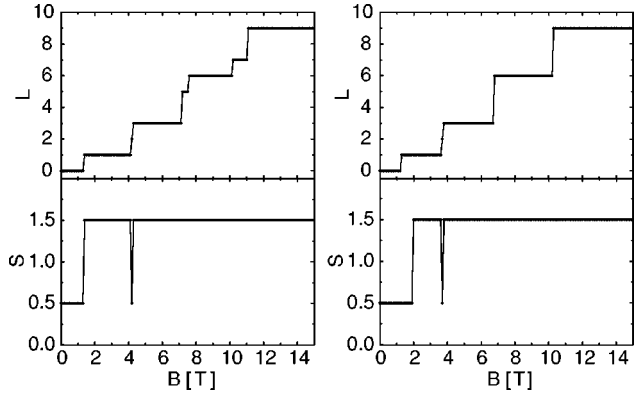

FIG. 5. The total angular momentum L and the total spin S of a double dot containing three electrons with confinement energy $\hbar\omega_{0+}=\hbar\omega_{0+}=3.0$ meV and a layer separation $d=20$ nm. $\Delta_{\mathrm{SAS}}=0.2$ (0.6) meV for the left (right) panel.

separation d, or equivalently, the ratio of the intralayer and interlayer Coulomb interactions. Thus we have to check which of the magic number states can become true ground states.

We have done this in Fig. 5. Here we have also included the effect of spin degrees of freedom. Thus what we have plotted in the figure is the total spin as well as the total angular momentum of the ground state of the three-electron double dot against magnetic field for $\Delta_{\mathrm{SAS}}=0.2$ (0.6) meV in the left (right) panel. One finds that the magic number states for ($L=5$ and $S=\frac{3}{2}$) or ($L=7$ and $S=\frac{3}{2}$) become the absolute ground state for $B=7.2$–7.5 T or $B=10.2$–11.0 T, respectively, for $\Delta_{\mathrm{SAS}}=0.2$ meV. On the other hand, the magic numbers $L=5$ and 7 are washed out when Δ_{SAS} is increased to 0.6 meV.

B. Four-electron double dots

The crossover between the dominant intralayer correlation and dominant interlayer correlation also exists in four-electron systems. The total angular momentum and the total spin of the ground state of four electrons are shown in Fig. 6. The system is fully spin polarized for $B\geqslant 3.2$ T, where the magic number orbital angular momentum evolves as L

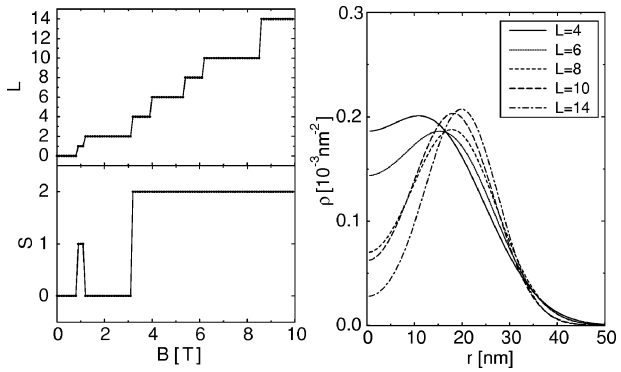

FIG. 6. Left: The total angular momentum L and the total spin S of a double dot containing four electrons with confinement energy $\hbar\omega_{0+}=\hbar\omega_{0-}=3.0$ meV. The layer separation is $d=20$ nm, and $\Delta_{\mathrm{SAS}}=0.6$ meV. Right: Charge density (ρ) per electron for each layer for typical ground states in the fully spin-polarized region, $B\geqslant 3.2$ T.

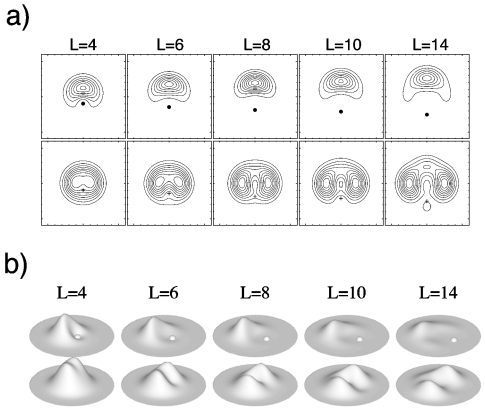

FIG. 7. (a): Contour plot of intralayer (upper panels) and interlayer (lower panels) pair-correlation functions, $P(\mathbf{r},\mathbf{r}_0)$, are displayed for each of the magic-L states in the true ground state for the four-electron double dot shown in Fig. 6, for appropriate values of B (in contrast to Fig. 4, where B is fixed). One electron (white sphere) is fixed in the upper layer at the place where the charge density is at maximum. Thus the total charge is 1 (2) in the upper (lower) layer, since we have 2 + 2 electrons, while we fix one electron in the upper layer. An area with the linear dimension of 12λ (λ: effective magnetic length) is displayed. The confinement energies, the layer separation d, and Δ_{SAS} are the same as in Fig. 6. (b) Bird's eye view plot of (a). A white sphere indicates the position of the fixed electron.

$=4$, 6, 8, 10, and 14. In this regime we can discuss the magic numbers without complications coming from real spins.

The charge density in Fig. 6 is single peaked for values of L up to 14. However, unlike the three-electron case, this does not imply that the correlation is developed within each layer. If we look at the pair-correlation function in Fig. 7, we can in fact see that the correlation is developed across the two layers. Since we have four electrons, we have now a tetrahedral configuration (with two electrons in the upper layer, and the other two in the lower layer in a staggered position) for all the magic number states.

As the magnetic field increases, the period of magic numbers changes from 2 [$L=(6+2)\times$integer] to 4 [$L=(6+4)\times$integer] as shown in the left panel of Fig. 6. The absence of the magic number $L=12$ is strong evidence for this change, because $L=12$ belongs only to the sequence $L=(6+2)\times$integer. The change of the period of the magic numbers corresponds to a crossover between dominant intralayer correlation and dominant interlayer correlation by analogy with three-electron systems, where the period of the magic numbers changes from 2 ($L=5$ and 7) to 3 ($L=9$ and 12), and $L=11$ is the missing magic number. The results for the pair-correlation function in Fig. 7 also show that interlayer correlation develops as L increases.

C. Crossover between intralayer and interlayer correlations

Intuitively the change in the correlation exemplified above for three and four electrons can be understood by considering the total energy. If the total angular momentum L is decreased at a fixed magnetic field, the lateral spatial extent ($\propto\sqrt{L}$) of the wave function is compressed, so that the mean electron separation a becomes comparable to the vertical

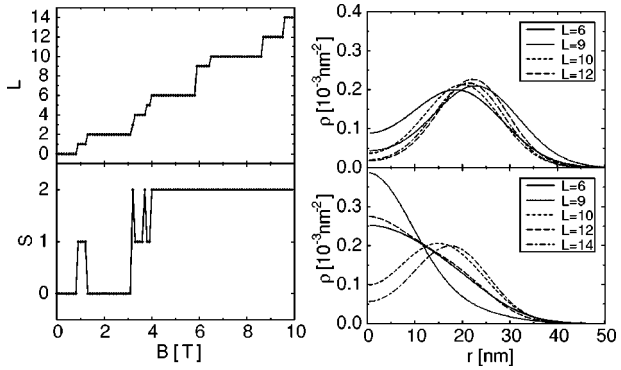

FIG. 8. Left: The total angular momentum L and the total spin S of a double dot containing four electrons with confinement energy $\hbar\omega_{0+}=3.0$ meV and $\hbar\omega_{0-}=3.3$ meV. The layer separation is $d=20$ nm, and $\Delta_{\mathrm{SAS}}=0.6$ meV. Right: Average charge densities (ρ) per electron for upper (lower) layer in the ground states are displayed in the upper (lower) panel for $L\geqslant 6$, for which the spins are fully polarized.

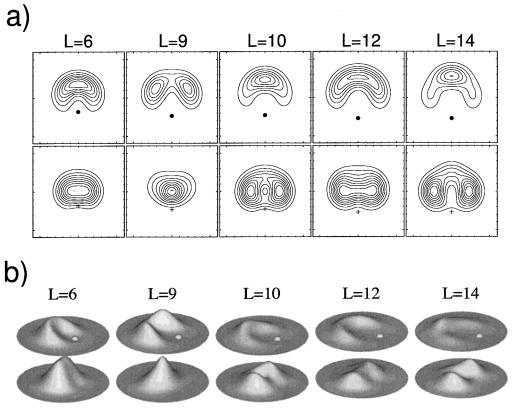

FIG. 9. Contour plot of intralayer (upper panels) and interlayer (lower) pair-correlation functions $P(\mathbf{r},\mathbf{r}_0)$ for the same ground states as shown in Fig. 8. One electron (white sphere) is fixed in the upper layer at the point where the charge density has a maximum. An area with the linear dimension of 12λ is displayed. The confinement energies, the layer separation d, Δ_{SAS}, and the magnetic field B are the same as in Fig. 8. (b) Bird's eye view plot of (a). A white sphere indicates the position of the fixed electron.

separation d of the layers. When the two layers are close enough, $d\ll a$, the system is effectively one layer, so that all the electrons are correlated (with a square configuration for the four-electron case) within each layer. In the opposite case of separated layers, $d\gg a$, the electrons in a, say, four-electron system should tend to minimize the energy by separating into two electrons in the upper layer and another two electrons in the lower, ending up with a tetrahedral configuration across the layers. This is because the typical intralayer Coulomb repulsion ($\propto 1/a$) becomes significantly greater than that of the interlayer Coulomb interaction ($\propto 1/\sqrt{a^2+d^2}$), so that the electrons will avoid each other as far as possible by ''sidetracking,'' i.e., by developing interlayer correlations. Such staggered configurations have to involve the mixing of symmetric and antisymmetric states across the two dots via the interlayer tunneling, and costs an energy Δ_{SAS}. This explains why the magic numbers tend to emerge for smaller Δ_{SAS}'s. Thus we can call the change in the nature of the electron correlation a crossover from a dominant intralayer correlation to a dominant interlayer correlation. Further, if L is increased, a becomes large and the interlayer and intralayer interactions become similar. Then the system is again effectively one layer, and this explains the tendency for new magic numbers to occur for smaller L. These qualitative arguments apply for any value of the magnetic field, but the magnetic field determines the overall length scale and hence the L value of the true ground state.

D. Effect of the pseudospin Zeeman energy

When the two layers have different confinement potentials, the difference plays the role of a Zeeman energy for the pseudospin,[17,30]

$$\varepsilon_{nl\sigma+}-\varepsilon_{nl\sigma-}=\tfrac{1}{2}(2n+1+|l|)\hbar(\Omega_+-\Omega_-), \qquad (10)$$

where $\Omega_\pm\equiv(\omega_c^2+4\omega_{0\pm}^2)^{1/2}$. The layer having the smaller confinement potential tends to accumulate charge, and this causes a charge density imbalance between the two layers as shown in Fig. 8 for a 10% difference in $\hbar\omega_{0+}=3.0$ meV, and $\hbar\omega_{0-}=3.3$ meV.[17] For four-electron systems, the Zeeman effect for pseudospin leads to a magic number which corresponds to tetrahedral-like charge correlations.[18]

Magic angular momenta and the total spin in this case are displayed in Fig. 8. We can see that the real spins are fully polarized for $B\geqslant 4$ T. Let us discuss this region in order to focus on the pseudospin. There the magic numbers are $L=6$, 9, 10, 12, and 14, and we notice that the magic numbers $L=9$ and 12 do not appear in system without the pseudospin Zeeman energy. In particular, $L=9$ belongs to neither the $L=(6+2)\times$integer nor $L=(6+4)\times$integer sequence. Instead it belongs to the $L=(6+3)\times$integer sequence, which implies a threefold symmetry in the charge correlation.

The average charge densities in the ground states are shown in Fig. 8 for both upper and lower layers. The densities for $L=6$, 9, and 12, which belong to the sequence $L=(6+3)\times$integer, are peaked at the center. If we look at the pair-correlation function in Fig. 9, the $L=9$ state is indeed seen to have a trigonal cone (3×1) configuration (while the $L=6$ state may be thought of as a mixture of twofold and trigonal configurations). The $L=12$ state belongs to both $L=(6+3)\times$integer and $L=(6+2)\times$integer sequences, so that its correlation is a mixture of conical (3×1) and tetrahedral (2×2) symmetries.

It would be interesting to compare our results with the phase diagram for the bulk bilayer FQH system obtained experimentally[31] or theoretically.[32] The picture in the bulk is that the quantum Hall state evolves, as Δ_{SAS} is decreased, from a tunneling-dominated state to a correlation-dominated one. The former is a fully occupied symmetric state (one-component state), while the latter is an interlayer-correlated Laughlin's liquid, Ψ_{331} (two-component) state.

To compare these with the dot states, however, is not straightforward. The bulk phase diagram is drawn against two dimensionless quantities d/l_B and $\Delta_{\mathrm{SAS}}/(e^2/\epsilon l_B)$, where $l_B\equiv(\hbar/m^*\omega_c)^{1/2}$ is the magnetic length. Because of the confining potential, the relevant length scale for dots becomes the effective magnetic length λ, with $\lambda^2=\hbar/m^*(\omega_c^2$

$+4\omega_0^2)^{1/2}$. With the parameters we have used $\lambda=(0.91\sim0.97)l_B$ for $B=(5-10)$ T. This yields $e^2/\epsilon\lambda=14.7$ meV for $B=10$ T, so that $\Delta_{\rm SAS}/(e^2/\epsilon\lambda)=0.01-0.04$ for the double dots considered here. The Landau-level filling ν, which is usually defined as

$$\nu=N(N-1)/2L$$

for a dot having N electrons, ranges from $\nu=\frac{3}{5}$ for $L=5$ to $\nu=\frac{1}{4}$ for $L=12$ for $N=3$. Although there is some attempt at extending the bulk phase diagram from the usually studied $\nu=1$ case to $\nu=1/(\text{odd integer})$,[13] the wide variation in ν and the fact that a change in B also changes λ complicate the comparison.

IV. FIR ABSORPTION

Now we move on to the FIR absorption spectrum. In a single dot with a parabolic confinement potential, the electron-electron interaction cannot affect the FIR absorption. This is dictated by Kohn's theorem,[33] originally conceived for translationally symmetric systems and later generalized to 2D dots with parabolic confinement in magnetic fields.[20,21] That is, long-wavelength electromagnetic radiations with electric field **E** couple to the dot via the dipole interaction

$$\mathcal{H}'=\sum_{i=1}^{N} e\mathbf{E}\cdot\mathbf{r}_i, \tag{11}$$

which depends only on the center-of-mass coordinate. In a single dot with parabolic confinement, the Hamiltonian separates into center-of-mass and relative (interaction) parts even in the presence of magnetic fields, and the latter is irrelevant to optical transitions. Recent optical measurements of quantum dots indeed exhibit absorption frequencies that are independent of the number of electrons and well fitted to the single-electron absorption spectrum.[34]

In contrast, the separation of the center-of-mass and relative parts does not occur in vertically coupled dots having different confinement potentials, even when they are both parabolic. This means that the Coulomb interaction can affect FIR absorption spectra.

To quantify the effect we have calculated the FIR absorption spectrum of vertically coupled dots from the matrix element of the perturbation Hamiltonian $\mathcal{H}'$ between the ground state and all the excited states. Before discussing the results, we comment on the applicability of this approach to real systems. One important question is the nature of the electric field **E** in small samples. Several authors have questioned the relation between the applied electric field and the internal electric field in mesoscopic systems,[35–37] with the general conclusion that depolarization effects are important. Therefore, we would have to calculate the internal electric field to obtain the absolute value of the absorption coefficient. In addition, a precise calculation of the absorption spectrum would require us to take account of other device properties that affect absorption, such as finite thickness of the individual dots and deviations from a parabolic potential, about which scant information is available. We therefore make the reasonable assumption that the internal electric field is uniform, and discuss only the absorption energy and the relative intensities of various transitions. This should be sufficient for our purpose of demonstrating that the FIR absorption of vertically coupled dots is affected by the electron correlation.

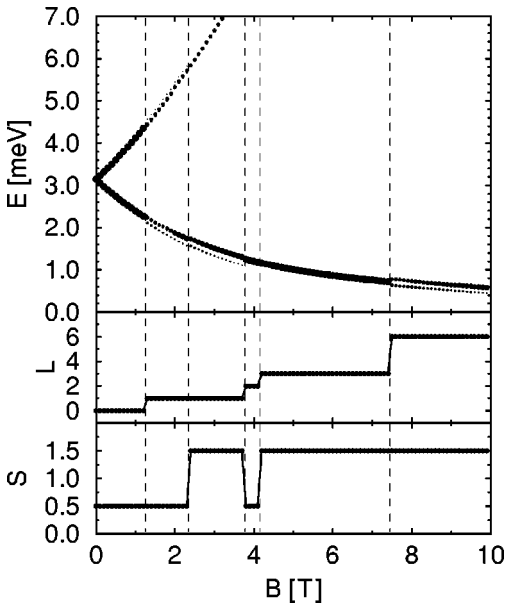

FIG. 10. FIR absorption spectrum (top panel), the total angular momentum (middle), and the total spin (bottom) of vertically coupled dots for $N=3$ electrons. $\hbar\omega_{0+}=3.0$ meV, $\hbar\omega_{0-}=3.3$ meV, the layer separation $d=20$ nm, and $\Delta_{\rm SAS}=0.6$ meV. The position of each filled circle gives the energy of the transition, while the size of the circle represents the relative intensity of the absorption. Vertical dashed lines are guides for the eye.

The FIR absorption spectrum consists of two branches: the upper branch for inter-Landau-level transitions, which approaches to the cyclotron frequency in the $B\rightarrow\infty$ limit; and the lower one for intra-Landau-level transitions. If we plot the position and intensity of the peaks in the FIR spectra along with the ground-state total angular momentum L and spin S (Figs. 10 and 11), we find a one-to-one correspondence between the magnetic fields at which the absorption line jumps and the magnetic fields at which the total angular momentum and/or the total spin of the ground state changes from one magic number state to another. Thus the transitions should be directly observable in the FIR absorption spectrum. The figure also shows that the absorption intensity ($\propto$ square of the matrix element) is not monotonic. We have also displayed the FIR spectra for a four-electron system, which again exhibit similar jumps. The magnitudes of the jumps, obtained assuming a confining potential asymmetry of 10%, is a few tenths of a meV. We believe they should be observable and the effect could probably be enhanced by making a double dot with greater potential asymmetry.

V. SPIN BLOCKADE

We now turn to the possibility of a spin blockade. It has been known for some time that the Coulomb blockade occurs in mesoscopic systems such as quantum dots. This is a combined effect of the discreteness of energy levels and the electron-electron interaction (charging energy). Weimann,

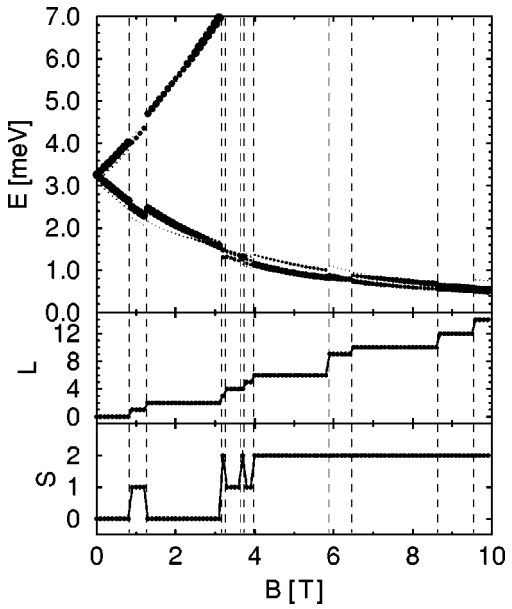

FIG. 11. The FIR absorption spectrum (top panel), total angular momentum (middle), and total spin (bottom) of vertically coupled dots for $N=4$ electrons are shown in the left (right) panel. $\hbar\omega_{0+}=3.0$ meV, $\hbar\omega_{0-}=3.3$ meV, the layer separation $d=20$ nm, and $\Delta_{\mathrm{SAS}}=0.6$ meV. The position of each filled circle gives the energy of the transition, while the size of the circle represents the relative intensity of absorption. Vertical dashed lines are guides for the eye.

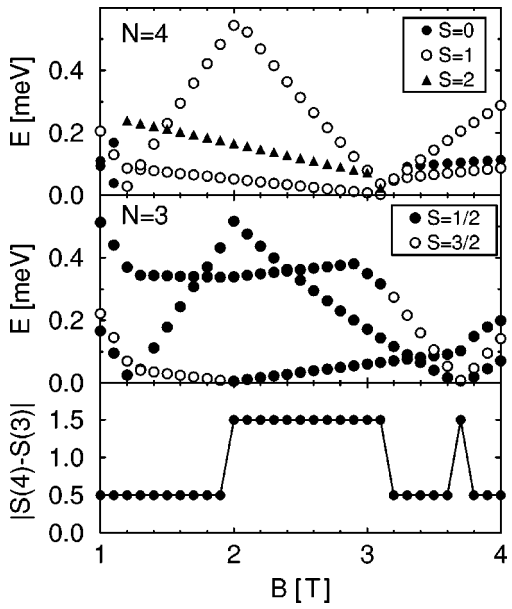

FIG. 12. Top (middle): Low-lying excitation energies for $N=4$ ($N=3$) double dots. Bottom: The absolute value of the difference, $|S(4)-S(3)|$, in the total spin for $N=4$ and 3 double dots. $\hbar\omega_{0+}=\hbar\omega_{0-}=3.0$ meV, the layer separation $d=20$ nm, and $\Delta_{\mathrm{SAS}}=0.6$ meV.

Hausler, and Kramer then suggested that, if the total spin differs by more than $\frac{1}{2}$ in the ground states for N and $(N-1)$ electrons, i.e.,

$$|S(N)-S(N-1)|>\tfrac{1}{2}, \tag{12}$$

the transport of an electron through the dot is blocked, and this should cause missing peaks in the conductance due to single electron tunneling at zero temperature. This is called the spin blockade,[38,39] and has been studied theoretically in the case of no magnetic field, where we can apply the Hund's coupling picture.[4] However, we cannot satisfy the spin-blockade condition for circular quantum dots with parabolic confinement potential in this case, so that some modifications such as an anharmonicity in the confinement potential[40] or rectangular hard-wall shape confinement potential[38] have to be introduced.

Now our idea here is to exploit the manifestation of the electron correlation in the total spin in the present system. We have in fact seen that electron correlation dominates the total spin (S) of the ground state in a peculiar manner, as shown in Figs. 5, 6, and 8, which comes from the fact that the magic values of L and S are linked. This is in a sense no surprise, since the total spin dictates, through Pauli's exclusion principle, the way in which the electrons can correlate, while the magic numbers in L come from the electron correlation as one of the authors showed from the electron molecule picture for single-layer quantum dots.

The correlation effect in fact happens when the typical Coulomb energy is much greater than the single-electron level spacing. Effects of electron correlation on the spin states via Pauli's principle are known to occur in ordinary correlated electron systems such as the Hubbard model, but the present case is a peculiar manifestation in strong magnetic fields.

Here we propose to utilize this electron-correlation effect to realize a spin blockade. For that we can look at our results for S to see if the spin-blockade condition [Eq. (12)] is satisfied in some regions of B. In addition, if there are low-lying excited states through which an electron can be transferred, the blockade will not occur except at the temperatures lower than the excitation energy. Thus we have to study the energies of excited states as well. We have plotted these along with $|S(4)-S(3)|$ for double dots that contain three or four electrons with the same parabolic confinement potential for both layers. The total angular momentum and the total spin of the ground state are shown in the right panel of Fig. 5 for $N=3$, and in the left panel of Fig. 6 for $N=4$.

The difference between the total spin of three- and four-electron systems, shown in the bottom panel of Fig. 12, indicates that the spin-blockade condition $|S(4)-S(3)|>\frac{1}{2}$ is satisfied for $2.0\leqslant B\leqslant 3.1$ T and $B=3.7$ T. In that region the excitation energies (top and middle panels of Fig. 12) for $N=3$ and 4 are of the order of 0.05 meV, which is unfortunately only half the typical experimental resolution $\simeq 0.1$ meV. However, it is possible to enhance the excitation energy by tuning $\hbar\omega_0$, d, or Δ_{SAS}. For instance, a double dot with $\hbar\omega_0=6.0$ meV, $d=16$ nm, and $\Delta_{\mathrm{SAS}}=1.2$ meV has an excitation energy of about 0.12 meV, which should be large enough to cause an experimentally observable spin blockade between $N=2$ and 3.[41] We also notice a level crossing between the second and third excited states around $B=2.4$ T for $N=3$, which should appear in the addition energy spectra.

VI. CONCLUSION

We have studied double-quantum-dot systems by using exact diagonalization including spin degrees of freedom and

higher Landau levels. We have found magic numbers specific to double dots, and shown that they are related to the symmetry of charge correlations. In addition, we have shown that we can change the charge correlation, total angular momentum, and total spin by varying the strength of the magnetic field *B*. These changes have been shown to affect the optical-absorption spectrum and single-electron tunneling. For the optical-absorption spectrum, we found that because of the breakdown of Kohn's theorem, the spectra differ from that of noninteracting system with splitting and jumps in the optical-absorption spectrum. The magnetic field where the spectrum has jumps is the field where the total angular momentum and/or the total spin of the ground-state shift from magic value to another. In the case of single-electron tunneling, we have shown that the tunneling is blocked because of the spin-selection rule—the spin blockade, in some magnetic-field regions.

ACKNOWLEDGMENTS

We wish to thank Professor Seigo Tarucha and Dr. David Guy Austing for a number of illuminating discussions.

[1] P. A. Maksym, Phys. Rev. B **53**, 10 871 (1996).
[2] H. Imamura, P. Maksym, and H. Aoki, Physica B **249-251**, 214 (1998).
[3] U. Merkt, Physica B **189**, 165 (1993).
[4] S. Tarucha, D. G. Austing, and T. Honda, Phys. Rev. Lett. **77**, 3613 (1996).
[5] R. C. Ashoori, H. L. Stormer, J. S. Weiner, L. N. Pfeiffer, S. J. Pearton, K. W. Baldwin, and K. W. West, Phys. Rev. Lett. **68**, 3088 (1992).
[6] R. C. Ashoori, H. L. Stormer, J. S. Weiner, L. N. Pfeiffer, K. W. Baldwin, and K. W. West, Phys. Rev. Lett. **71**, 613 (1993).
[7] M. Wagner, U. Merkt, and A. Chaplik, Phys. Rev. B **45**, 1951 (1992).
[8] *The Quantum Hall Effect*, 2nd ed., edited by R. E. Prange and S. M. Girvin (Springer-Verlag, New York, 1990).
[9] *Quantum Hall Effect*, 2nd ed., edited by T. Chakraborty and P. Pietiläinen (Springer-Verlag, New York, 1995).
[10] *Perspectives in Quantum Hall Effects*, edited by S. Das Sarma and A. Pinczuk (Wiley, New York, 1997).
[11] J. Eisenstein, G. S. Boebinger, L. N. Pfeiffer, K. W. West, and Song He, Phys. Rev. Lett. **68**, 1383 (1992).
[12] K. Moon, H. Mori, Kun Yang, S. M. Girvin, A. H. MacDonald, L. Zheng, D. Yoshioka, and Shou-Cheng Zhang, Phys. Rev. B **51**, 5138 (1995).
[13] T. Nakajima and H. Aoki, Phys. Rev. B **51**, 7874 (1995).
[14] T. Nakajima and H. Aoki, Phys. Rev. B **52**, 13 780 (1995).
[15] Y. W. Suen, L. W. Engel, M. B. Santos, M. Shayegan, and D. C. Tsui, Phys. Rev. Lett. **68**, 1379 (1992).
[16] D. Yoshioka, A. H. MacDonald, and S. M. Girvin, Phys. Rev. B **39**, 1932 (1989).
[17] H. Imamura, P. A. Maksym, and H. Aoki, Phys. Rev. B **53**, 12 613 (1996).
[18] P. A. Maksym, H. Imamura, and H. Aoki, in *Proceedings of the 23rd International Conference on the Physics of Semiconductors*, edited by M. Scheffler and R. Zimmermann (World Scientific, Singapore, 1996), p. 1613.
[19] H. Imamura, H. Aoki, and P. A. Maksym, Phys. Rev. B **57**, 4257 (1998).
[20] L. Brey, N. F. Johnson, and B. I. Halperin, Phys. Rev. B **40**, 10 647 (1989).
[21] P. A. Maksym and T. Chakraborty, Phys. Rev. Lett. **65**, 108 (1990).
[22] N. F. Johnson, J. Phys. Condens. Matter **7**, 965 (1995).
[23] D. G. Austing, T. Honda, and S. Tarucha, Jpn. J. Appl. Phys., Part 1 **36**, 1667 (1997).
[24] V. Fock, Z. Phys. **47**, 466 (1928).
[25] C. G. Darwin, Proc. Cambridge Philos. Soc. **27**, 86 (1930).
[26] R. B. Laughlin, Phys. Rev. B **27**, 3383 (1983).
[27] S. M. Girvin and T. Jach, Phys. Rev. B **28**, 4506 (1983).
[28] R. J. Galejs, Phys. Rev. B **35**, 6240 (1987).
[29] M. Stone, H. W. Wyld, and R. L. Schult, Phys. Rev. B **45**, 14 156 (1992).
[30] J. J. Palacios and P. Hawrylak, Phys. Rev. B **51**, 1769 (1995).
[31] G. S. Boebinger, H. W. Jiang, L. N. Pfeiffer, and K. W. West, Phys. Rev. Lett. **64**, 1793 (1990).
[32] A. H. MacDonald, P. M. Platzman, and G. S. Boebinger, Phys. Rev. Lett. **65**, 775 (1990).
[33] W. Kohn, Phys. Rev. **123**, 1242 (1961).
[34] B. Meurer, D. Heitmann, and K. Ploog, Phys. Rev. Lett. **68**, 1371 (1992).
[35] J. A. A. J. Pernboom, P. Wyder, and F. Meier, Phys. Rep. **78**, 173 (1981).
[36] K. Cho, Prog. Theor. Phys. Suppl. **106**, 225 (1991).
[37] O. Keller and T. Garm, Phys. Rev. B **52**, 4670 (1995).
[38] D. Weinmann, W. Hausler, and B. Kramer, Phys. Rev. Lett. **74**, 984 (1995).
[39] Y. Tanaka and H. Akera, Phys. Rev. B **44**, 3901 (1996).
[40] M. Eto, J. Appl. Phys. **36**, 3924 (1997).
[41] H. Imamura, P. A. Maksym, and H. Aoki, Phys. Rev. B **57**, R12 808 (1998).